Bortezomib-Induced Survival Signals and Genes in Human Proximal Tubular Cells

Rita Sarközi, Paul Perco, Kathrin Hochegger, Julia Enrich, Martin Wiesinger,

Markus Pirklbauer, Susanne Eder, Michael Rudnicki, Alexander R. Rosenkranz,

Bernd Mayer, Gert Mayer, and Herbert Schramek

Division of Nephrology and Hypertension, Department of Internal Medicine IV, Innsbruck

Medical University, Innsbruck, Austria (R.S., K.H., J.E., M.P., S.E., M.R., A.R.R., G.M.,

H.S.); and emergentec biodevelopment GmbH, Vienna, Austria (P.P., M.W., B.M.)

1

JPET #142604

Running Title: Bortezomib-induced protection pathways and genes

Address correspondence to: Dr. Herbert Schramek, Division of Nephrology and Hypertension, Department of Internal Medicine IV, Innsbruck Medical University, Anichstrasse 35, A-6020 Innsbruck, Austria. Phone: +43 (0) 50504 27316; Fax: +43 (0) 50504 25857;

E-mail: herbert.schramek@i-med.ac.at

Document statistics:

Number of …

Text pages :	32
Tables:	0
Figures:	10
References:	40
Words in Abstract:	220
Words in Introduction:	716
Words in Discussion:	1482

List of non-standard abbreviations:

BAG	Bcl-2-associated athanogene
BH3	Bcl-2 homology domain 3
BPE	bovine pituitary extract
DEG	differentially expressed genes
EGF	epidermal growth factor
ERK	extracellular signal-regulated kinase
FBS	fetal bovine serum
GMC	glomerular mesangial cells
HGF	hepatocyte growth factor
HSP	heat shock protein
JNK	c-Jun-N-terminal kinase
MAPK	mitogen-activated protein kinase

JPET #142604

MEK	MAPK ERK kinase
MM	multiple myeloma
NF-κB	nuclear factor-κB
PI3K	phosphatidylinositol 3-kinase
PKB	protein kinase B
PTC	proximal tubular epithelial cells

Recommended section assigment:

Cellular and Molecular

ABSTRACT

Bortezomib has recently been introduced in the therapy of multiple myeloma (MM), a disease which is frequently associated with progressive renal failure. As bortezomib-based therapy has been reported to lead to a rapid recovery of kidney function in patients with MM, we decided to study its direct effects in proximal tubular epithelial cells (PTC) when compared with glomerular mesangial cells (GMC). After 24 h of stimulation, 50 nM bortezomib led to a 6.37-fold induction of apoptosis and markedly activated caspase-9 and caspase-3 in GMC but not in PTC. In PTC but not in GMC, bortezomib led to a strong time-dependent degradation of IκB-α as well as to a long-lasting phosphorylation of both NF-κBp65 and ERK1/2. Microarray analysis in bortezomib-treated PTC revealed a time-dependent predominance of anti-apoptotic genes when compared with pro-apoptotic genes. 50 nM bortezomib induced Hsp70 mRNA and protein levels in PTC, while basal and bortezomib-stimulated Hsp70 protein expression was much weaker in GMC. Moreover, bortezomib induced BAG3 mRNA and protein expression but inhibited BAG5 mRNA levels in PTC. These data suggest that the reduced susceptibility of PTC to bortezomib-induced cell apoptosis is due to cell type-specific effects of this compound on apoptosis/survival genes and pathways. The concept of bortezomib representing a blocker of both NF-κB activation and cell survival should be carefully examined in particular renal cell types.

Introduction

The 26S proteasome, a multicatalytic protease complex expressed in the nucleus and cytoplasm of all eukaryotic cells, has traditionally been viewed as a recycler of damaged or misfolded proteins responsible for most nonlysosomal intracellular protein degradation. However, emerging data have revealed that besides degrading proteins tagged with ubiquitin, the proteasome plays a more varied and decisive role in cellular regulation than previously imagined (Chiechanover and Schwartz, 1998; DeMartino and Gillette, 2007). Aside from its role as a protease, the proteasome also functions nonproteolytically in a variety of cellular processes including transcription, DNA repair, and chromatin remodeling (DeMartino and Gillette, 2007). Furthermore, the normal degradation of proteins is crucial for maintenance of cellular homeostasis, and the proteasome plays a critical role in modulating intracellular levels of a variety of proteins such as tumor suppressors, oncogenes, and proteins that are involved in cell cycle regulation (Chiechanover and Schwartz, 1998). This is one reason why the 26S proteasome has received much attention as a potential therapeutic target, and why various proteasome inhibitors have been actively studied for their antitumor effects (Adams, 2002).

Bortezomib (PS-341, Velcade®), a boronic acid dipeptide, is a potent, selective and reversible proteasome inhibitor that has been shown to induce cell death in many tumor models, including prostate, colon, and pancreatic cancer as well as multiple myeloma (MM) (Frankel et al., 2000; Cusack et al., 2001; Hideshima et al., 2001). Of these malignant diseases, the hematologic neoplasia MM is characterized by monoclonal proliferation of bone marrow plasma cells leading to a number of organ dysfunctions and symptoms such as bone pain or fracture, susceptibility to infection, anemia, and renal failure. Approximately 20% to 40% of newly diagnosed MM patients develop renal impairment, with up to 13% having renal failure requiring dialysis (Chanan-Khan et al., 2007; Kastritis et al., 2007). Several studies

have shown that the severity of renal impairment significantly affects the prognosis of patients with MM (Chanan-Khan et al., 2007). With supportive measures and antimyeloma treatment, renal failure is reversible in 25% to 58% of patients (Kastritis et al., 2007). New agents such as bortezomib, either as a monotherapy or in combination with dexamethasone, have been very efficient in newly diagnosed MM patients (Jagannath et al., 2005). Bortezomib can be safely used in relapsed patients with renal impairment and two preliminary reports have been published recently showing that bortezomib-combination therapy led to a reversal of acute multiple myeloma-induced renal failure (Mohrbacher et al., 2005; Ostermann et al., 2006). Additional studies revealed reversibility of renal failure in newly diagnosed MM patients treated with high-dose dexamethasone containing regimens and a more rapid improvement of renal function in the presence of bortezomib (Nozza et al., 2006; Kastritis et al., 2007). These findings are in line with a recent retrospective multicenter study performed with MM patients requiring dialysis for advanced renal failure, which suggested that bortezomib therapy is a well-tolerated, effective option in the subgroup of MM patients with severe renal dysfunction (Chanan-Khan et al., 2007).

Albeit these clinical results are encouraging, there is still little information available about the direct cellular effects of bortezomib treatment in kidneys and the cell type-specific intracellular mechanisms induced by this proteasome inhibitor. These are important questions, because, for reasons that remain to be fully elucidated, some cell types seem to be more sensitive to the effects of bortezomib-induced proteasome inhibition than others (Adams, 2002). We, therefore, first hypothesized that bortezomib treatment is associated with the induction of mechanisms leading to both apoptosis/cell death as well as cell survival. Secondly, the final cellular outcome of bortezomib administration might largely depend on the specific cell type affected by this treatment. As proximal tubular injury is the most common mode of renal involvement in MM (Batuman, 2007), and in order to gain insight into the molecular mechanisms affected by bortezomib along the proximal tubule, we examined

6

time-dependent global gene expression profiles in bortezomib-treated human proximal tubular cells (PTC). Moreover, we investigated anti-apoptotic/cell survival pathways and pro-apoptotic/cell death pathways in epithelial PTC when compared with renal glomerular cells of mesenchymal origin, namely glomerular mesangial cells (GMC). Here, we report that bortezomib is able to modulate renal cellular function in a cell type-specific manner. Bortezomib affects a set of intracellular signaling events and genes, which are likely to protect these PTC from apoptosis rather than inducing apoptosis.

Methods

Chemicals and Reagents. Cell culture reagents were obtained from Gibco (Life Technologies, Lofer, Austria). Bortezomib ($C_{19}H_{25}BN_4O_4$, [(1*R*)-3-methyl-1-[[(2*S*)-1-oxo-3-phenyl-2-[(pyrazinylcarbonyl)amino]propyl]amino]butyl] boronic acid, PS-341, Velcade®) was kindly provided by Janssen-Cilag Pharma, Vienna, Austria. Unless otherwise indicated, all other reagents were obtained from Sigma (St. Louis, MO).

Cell culture. Human proximal tubular cells (PTC) HK-2 (human kidney-2), representing a HPV 16 E6/E7-immortalized human PTC line from normal adult human kidney, from passage 20-35 were cultured in Keratinocyte-Serum Free Medium (KSFM) containing 10% fetal bovine serum (FBS), 5 ng/ml recombinant epidermal growth factor (rEGF), 0.05 mg/ml bovine pituitary extract (BPE), 100 units/ml penicillin, and 100 μg/ml streptomycin (Sarközi et al., 2007). Rat glomerular mesangial cells (GMC) from passage 25-40 were maintained in RPMI 1640 medium supplemented with 10% FCS, 5 ng/ml each of insulin (I), and transferrin (T), and 5 μg/ml selenite (S), 100 units/ml penicillin, and 100 μg/ml streptomycin (Schramek et al., 1996). Wild-type LLC-PK$_1$ cells, representing a proximal tubular epithelial cell line derived from the pig kidney, were used from passages 178-185. They were grown in Eagle's minimal essential medium (MEM) supplemented with 100 units/ml penicillin, 100 μg/ml streptomycin, 1.2 mg/ml NaHCO$_3$, and 5% FBS, and split at a 1:10 ratio, once a week (Schramek et al., 1993). All cells were cultured at 37°C in a humidified 5% CO$_2$ atmosphere and, after growth to subconfluent state, they were washed once, made quiescent by incubation in serum- and supplement-free medium for 48 h, and then used for experiments. Stimulations with bortezomib were performed in the absence of serum and any other growth supplements.

Flow cytometric DNA analysis. PTC, LLC-PK$_1$ and GMC were made quiescent by incubation in serum- and supplement-free medium for 24 h, and then either left unstimulated or stimulated with 50 nM bortezomib in the absence of serum and any other growth supplements for 24 h. For flow cytometric analysis of apoptosis and necrosis, PTC, LLC-PK$_1$ and GMC were stained with a FITC-conjugated Annexin-V (Alexis, Carlsbad, CA, USA) and propidium iodide (Molecular Probes Eugene, Oregon, USA) for 10 minutes. Flow cytometry was performed using an Epics XL-MCL Flow

Cytometry System (Beckman Coulter Fullerton, CA, USA). Data were collected from at least 10,000

events. Bortezomib did not increase autofluorescence of the cell populations tested (data not shown).

Western blot analysis. Whole cell lysates were prepared using ice-cold RIPA lysis buffer (50

mM Tris·HCl, pH 7.5, 150 mM NaCl, 50 mM NaF, 5 mM EDTA, 0.5% deoxycholic acid, 40 mM β-

glycerophosphate, 1 mM sodium orthovanadate, 10% protease inhibitor cocktail for mammalian

tissues (Sigma, St. Louis, MO), 0.1% SDS, 1% Triton X-100). Protein matched samples were

subjected to SDS-polyacrylamide gel electrophoresis and than transferred to a polyvinylidene

difluoride microporous membrane (Millipore, Bedford, MA). Immunoblotting was performed as

described previously (Schramek et al., 1996; Sarközi et al., 2007). The following primary antibodies

were applied: cleaved-caspase-9 (Asp315), cleaved-caspase-3 (Asp175), phospho-NF-κB p65

(Ser536), phospho-p44/42 MAP Kinase (all from Cell Signaling Technology, Beverly, MA), NF-κB

p65, IκB-α, AKT1/2/3, phospho-Akt1/2/3 (Ser473)-R, ERK2, Hsp 70 (W27) (all from Santa Cruz

Biotechnology, Santa Cruz, CA), β-actin (Sigma Chemicals, St. Louis, MO), BAG3 (Alexis

Biochemicals, San Diego, CA).

Microarray hybridization and data analysis. We used human exonic evidence based

oligonucleotide (HEEBO) arrays from the Stanford Functional Genomics Facility

(http://www.microarray.org/sfgf/heebo.do). Total cellular RNA (*vide infra*) was reverse transcribed

using CyScribe cDNA Post Labelling Kit (GE Healthcare life sciences, Piscataway, NJ, USA). RNA

from bortezomib-stimulated cells was labelled with Cy-5 (red) and RNA from unstimulated control

experiments was labelled with Cy-3 (green). For each of the four different time points (4, 8, 16, and 32

h) a co-hybridization of Cy-5- and Cy-3-labelled reverse transcribed RNA was performed in biological

duplicates. Arrays were scanned with the Axon GenePix 4000B microarray scanner and the images

were analyzed with GenePix 6.0 software (Axon Instruments, Union City, CA, USA). Raw data as

well as array images were transferred to the Stanford Microarray Database (SMD) for data storage and

data pre-processing (http://genome-www5.stanford.edu/MicroArray/SMD). All experiments were

performed according to the MIAME (Minimum Information About a Microarray Experiment)

guidelines (Brazma et al., 2001). Mean log2 R/G values were used for analysis and only spots with

intensity values greater than 1.5 times the background values in either channel were considered for

analysis. 32083 of the 36293 retrieved spots were mapped to HGNC Gene Symbols. The other 4210 spots represented ESTs and hypothetical proteins.

Functional gene categorization was based on gene ontology terms which were assigned to all annotated genes on the chip using the GO package from the Bioconductor R module. The set of genes associated with apoptosis was extracted and gene expression values of those genes further analyzed. Values of different clones assigned to a single gene cluster were averaged and genes showing a fold-change of at least two in either direction in both replicate arrays at any time point were defined as differentially expressed.

To further evaluate the contribution of DEGs to anti- and pro-apoptotic processes, we determined the numbers of DEGs assigned to the respective gene ontology categories and compared those numbers to the background distribution of the apoptosis associated reference gene set on the chip.

RNA isolation and real-time PCR. Total cellular RNA was extracted using TRI Reagent (molecular Research Center, Cincinnati, OH). RNA quantity was estimated by spectrophotometric analysis. Reverse transcription was performed using 2 μg total RNA, 1 μM random hexanucleotides as primer (Roche Diagnostics, Indianapolis, IN), and Omniscript Reverse Transcriptase (Qiagen, Valencia, CA) according to the manufacturer's instructions.

Real-time PCR was performed using 2 μl of cDNA template from the RT reaction, 1x TaqMan Universal PCR Master Mix (Applied Biosystems, Foster City, CA) and premade TaqMan Gene Expression Assays (human GAPDH (Hs99999905m1), human BAG3 (Hs00188713m1) and human BAG5 (Hs00191644m1), Applied Biosystems, Foster City, CA) according to the manufacturer's instructions. Relative changes in gene expression (fold change) were calculated using the $2^{-\Delta\Delta CT}$ Method described by Livak and Schmittgen (Livak and Schmittgen, 2001).

Statistical analyses. Two-sided t-tests were used to assess the significance of differences of bortezomib administration on the percentage of apoptotic as well as necrotic cells in PTC and GMC when compared with untreated cells. Percent values of apoptotic cells are expressed as mean ± SEM.

10

Results

Proximal Tubular Cells (PTC) are Less Sensitive to Bortezomib-induced Apoptosis when compared with Glomerular Mesangial Cells (GMC). Bortezomib, which is a reversible inhibitor of the chymotrypsin-like activity of 26S proteasome, behaves as an efficient apoptotic agent in a number of tumor cells and has therefore been introduced in the therapy of MM (Hideshima et al., 2001). However, it has been noted earlier that one identical concentration of proteasome inhibitor has divergent effects on different cell types. Whereas proteasome inhibition induces apoptosis in rapidly proliferating tumor cells, the opposite response – protection from apoptosis – has been observed in differentiated and quiescent cells (Wojcik, 1999; Meiners et al., 2008). As no information about direct effects of bortezomib in renal cells is available to date and as the final cellular outcome of bortezomib administration might largely depend on both drug concentration and the specific cell type affected by this treatment, we first studied bortezomib-induced apoptosis/necrosis in PTC when compared with GMC utilizing FACS analysis following annexin V/propidium iodide staining. After 24 h of stimulation, 50 nM bortezomib led to a highly significant, 6.37-fold induction of apoptosis in GMC but not in PTC (Fig. 1A). GMC apoptosis increased from $2.13 \pm 0.2\%$ in unstimulated controls to $13.56 \pm 2.22\%$ in bortezomib-stimulated cells ($n = 12$; $p < 0.0001$). In contrast, PTC apoptosis showed only a slight 1.56-fold increase from $2.98 \pm 0.8\%$ in unstimulated cells to $4.66 \pm 1.43\%$ in bortezomib-treated cells ($n = 11$; $p = 0.316$). In parallel, bortezomib led to a similar induction of necrosis after 24 h in both cell types (Fig. 1B). Bortezomib stimulated necrosis 2.69-fold in PTC (from $4.31 \pm 0.68\%$ to $11.61 \pm 1.16\%$; $n = 11$; $p < 0.0001$) and 2.74-fold in GMC (from $6.19 \pm 1.36\%$ to $16.98 \pm 1.75\%$; $n = 12$; $p < 0.0001$) (Fig. 1). Representative dotblots of Annexin-V/propidium iodide staining of PTC and GMC are depicted in Figs. 1C and 1D, respectively. GMC display increased fractions of early apoptotic Annexin-V positive cells and necrotic propidium iodide positive cells after

11

treatment with bortezomib (Fig. 1D). In contrast, PTC show only a slight increase in both the late apoptotic double positive population and the necrotic propidium iodide positive population (Fig. 1C). When compared with untreated PTC, no difference in the early apoptotic Annexin-V positive cell population is visible after bortezomib administration. These results from FACS analysis are corroborated by the finding that bortezomib led to a strong activation of caspase-9 and caspase-3 in GMC (Fig. 2). 50 nM bortezomib induced a time-dependent cleavage of caspase-9 (Fig. 2 upper panel) and caspase-3 (Fig. 2 lower panel) in GMC, which started after 16 h and 8 h, respectively, and which was highest after 36 h. In contrast, only slight degradation of caspase-9 and caspase-3 was detected under identical experimental conditions in PTC (Fig. 2). In these cells, faint activation of caspase-9 could be detected between 8 hrs and 36 hrs after bortezomib administration (Fig. 2 upper panel), while a minor caspase-3 cleavage band was visible in bortezomib-treated PTC lysates after 36 h of stimulation only (Fig. 2 lower panel). In contrast to GMC, only a faint cleaved-caspase-3 band was detectable after 24 h of bortezomib administration in LLC-PK$_1$ cells, which represents a proximal tubular cell line derived from pig (Fig. 4). Similar to PTC, proximal tubular LLC-PK$_1$ cells showed a low susceptibility to bortezomib-induced cell death. After 24 h of stimulation, LLC-PK$_1$ cell apoptosis was increased from $1.56 \pm 0.89\%$ in unstimulated cells to $4.24 \pm 0.94\%$ in bortezomib-treated cells ($n = 8$; $p = 0.015$). Necrosis showed only a marginal induction from $3.33 \pm 0.58\%$ in unstimulated controls to $4.48 \pm 0.27\%$ in bortezomib-stimulated cells ($n = 8$; $p = 0.093$). These results together suggest that the proximal tubular epithelial cell lines HK-2 and LLC-PK$_1$ are less susceptible to bortezomib-induced apoptosis when compared with mesenchymal GMC.

Bortezomib Induces Long-lasting NFκBp65 Phosphorylation on Serine 536 in PTC but not in GMC. Nuclear factor (NF)-κB comprises a family of at least five proteins, which all contain a Rel homology domain mediating DNA binding, dimerization, and interaction with inhibitory factors known as IκB proteins (Perkins, 2007). The canonical NF-κB complex

12

represents a heterodimer composed of p50 and p65 subunits and regulates many physiological

processes, including cell death, apoptosis, adhesion and proliferation (Perkins, 2007).

Proteasome inhibitors have been reported to block IκB degradation, thereby sequestering NF-

κB in the cytoplasm and downregulating its transcriptional activity (Traenckner et al., 1994).

In many cell types apoptosis induced by administration of proteasome inhibitors is associated

with both accumulation of IκB-α and inhibition of NF-κB activity (Dai et al., 2003; An et al.,

2004). As PTC seem to be more resistant to bortezomib-induced cell apoptosis and as the

drugs effect on NF-κB activation probably depends on the nature and the cellular context of

its induction we next studied bortezomibs effects on NF-κB in PTC and LLC-PK$_1$ when

compared with GMC. Administration of 50 nM bortezomib led to a time-dependent reduction

of IκBα protein expression in PTC (Fig. 3). Bortezomib-induced IκB-α degradation in PTC

started after 8 h and was maximal after 36 h. GMC showed a stronger basal IκB-α protein

expression when compared with PTC and did not show a substantial bortezomib-induced

degradation during the time points investigated (Fig. 3, upper panel). In parallel bortezomib

(50 nM) time-dependently stimulated NF-κBp65 phosphorylation at serine 536 in PTC and in

GMC (Fig. 3, middle panel). In PTC strong bortezomib-induced p65 RelA phosphorylation

occurred as early as 8 h after administration and lasted for at least 36 h, while in GMC p65

RelA was only transiently phosphorylated after 8 h, which then again decreased to control

levels after 16 h before p65 RelA phosphorylation was almost abolished after 24 h and 36 h

(Fig. 3). No alterations in NF-κBp65 protein expression associated with bortezomib treatment

were detected in the two cell types investigated under these experimental conditions (Fig. 3,

lower panel). With respect to IκB-α degradation and NF-κBp65 phosphorylation at serine 536

similar results as described for PTC were obtained in proximal tubular LLC-PK$_1$ cells after 24

h of bortezomib administration (Fig. 4). As reduction of IκB-α protein levels and

phosphorylation of p65 RelA subunit on serine 536 is associated with increased NF-κB

transcriptional activity (Dolcet et al., 2006), these results suggest that in PTC and LLC-PK$_1$

13

bortezomib represents an activator of NF-κB rather than an inhibitor. In GMC, however, transient stimulation was followed by a strong inhibition of NF-κBp65 phosphorylation, which is consistent with the idea that bortezomib leads to a long-lasting activation of this cell survival/protection pathway in epithelial cells of proximal tubular origin such as PTC and LLC-PK$_1$ but not in GMC, which represent renal cells of mesenchymal origin.

Bortezomib Inhibits Akt/PKB Protein Expression in GMC but not in PTC. The serine/threonine kinase Akt, also known as protein kinase B (PKB), represents the crucial link between phosphatidylinositol 3-kinase (PI3K) and the prevention of apoptosis (Manning and Cantley, 2007). Akt is able to enhance the survival of cells by blocking the function of pro-apoptotic proteins and processes via various mechanisms. Akt activation, for example, prevents the processing of procaspase-9 through its inhibitory effects on the function and expression of several Bcl-2 homology domain 3 (BH3)-only proteins, which exert their pro-apoptotic effects by binding to and inactivating pro-survival Bcl-2 family members (Manning and Cantley, 2007). Akt has also been found to directly phosphorylate Ser196 on human procaspase-9, and this phosphorylation correlates with a decrease in the protease activity of caspase-9 *in vitro*. In addition, it has been reported that under some conditions the PI3K-Akt pathway can activate NF-κB survival signaling (Manning and Cantley, 2007). Thus, we next investigated the regulation of Akt/PKB in bortezomib-treated PTC when compared with GMC. As depicted in Fig. 5, Akt showed a high Ser 473 phosphorylation in PTC both under basal and bortezomib-stimulated conditions. In contrast, we did not detect Akt/PKB phosphorylation in GMC (Fig. 5, upper panel). Akt/PKB protein levels were equally expressed in both cell types under unstimulated control conditions (Fig. 5, middle panel). Interestingly, administration of 50 nM bortezomib led to a time-dependent inhibition of Akt protein expression in GMC, which started after 16 h and was maximal after 36 h (Fig. 5, middle panel). In contrast, no alteration of Akt protein expression was detected in bortezomib-treated PTC. Equal loading during these experiments was assured by the fact that

14

ß-actin protein expression was equal and unaffected by bortezomib treatment during all conditions tested (Fig. 5, lower panel).

Bortezomib Induces a Long-lasting ERK1/2 Phosphorylation in PTC but not in GMC. The mitogen-activated protein kinase family, especially the Raf-MEK1/2-ERK1/2 signaling module, represents another intracellular signaling system, which is important in the regulation of normal cell proliferation, cell survival and cell differentiation (Tori et al., 2006). Moreover, extracellular signal-regulated kinase (ERK) 1/2 signaling acts cooperatively with PI3K/Akt signaling in regulating growth factor-stimulated cell cycle progression (Tori et al., 2006). As ERK1/2 signaling could be also involved in the relative bortezomib resistance of PTC when compared with GMC we next investigated phosphorylation and expression of ERK1/2 in unstimulated and bortezomib-stimulated cells. After 24 h of PTC stimulation, bortezomib led to a concentration-dependent increase in ERK1/2 phosphorylation, which started at a concentration of 5 nM bortezomib and was maximal at 100 nM (data not shown). 50 nM bortezomib led to an induction of ERK1/2 phosphorylation in PTC, which started after 8 h and lasted for at least 36 h (Fig. 6). In GMC, bortezomib-stimulated, time-dependent ERK1/2 phosphorylation started after 8 h, was highest after 12 h but started to decrease after 16 h and already reached control levels after 36 h (Fig. 6). At the same time bortezomib did not affect ERK2 protein expression, neither in PTC, nor in GMC (Fig. 6, lower panel). Thus, the time-dependent decrease of NF-κBp65 phosphorylation, Akt protein expression and ERK1/2 phosphorylation in bortezomib-treated GMC is associated with the time-dependent activation of caspase-9 and caspase-3. In bortezomib-stimulated PTC, on the other hand, long-term activation of NF-κB and ERK1/2 as well as lack of Akt degradation could be involved in the relative resistance of these cells to apoptosis induction.

Bortezomib-mediated Differential Gene Expression in PTC: Evidence for a Time-dependent Predominance of Anti-apoptotic Genes when compared with Pro-apoptotic

Genes. In order to gain further insight into the molecular mechanisms affected by bortezomib along the proximal tubule, we next examined time-dependent global gene expression profiles in bortezomib-treated PTC utilizing oligonucleotide microarray analysis. After growth to a subconfluent state, PTC were washed once, made quiescent by incubation in serum- and supplement-free medium for 48 h, were then stimulated with 50 nM bortezomib for 4, 8, 16, 32 h and compared with unstimulated control cells. We identified 379 pro-apoptotic, 308 anti-apoptotic, and 538 apoptosis-related cDNA clones on the array mapping to 210 (33%), 157 (25%), and 261 (42%) unique genes based on HUGO Gene Nomenclature Committee (HGNC) Gene Symbols respectively (see webtable 1 at http://www.microarray.at section "Data" for a listing of GO terms and associated cDNA clones. Given are the Clone ID (CLID), the NCBI Gene ID (GeneID), the HGNC Gene Symbol (GeneSymbol), the Gene Name, as well as the apoptosis related gene ontology terms.). 181 of these in total 628 genes were differentially expressed at least at one time point after stimulation as depicted in webtable 2 at http://www.microarray.at section "Data". Values are given as log2 R/G, where R represents the borteomib treated gene array intensity values and G represents untreated intensity values. Genes are either designated as pro-apoptotic (+), anti-apoptotic (-), or apoptosis-related (o). The proportion of upregulated genes involved in anti-apoptotic processes (grey columns) when compared with those representing pro-apoptotic potential (black columns) steadily increased over time with a peak at 16 h after bortezomib treatment, while the number of down-regulated genes involved in pro- and anti-apoptosis was balanced (Fig. 7). The distribution of differentially expressed genes (DEGs) upregulated 16 h after treatment was significantly different from the reference set based on a chi-square test (p-value 0.0496). Ten DEGs (45% of upregulated genes) were involved in anti-apoptotic processes whereas only 3 (14%) had pro-apoptotic activity (Fig. 7). Upregulated anti-apoptotic genes included the Bcl-2-associated athanogene 3 (BAG3), the hepatocyte growth factor (HGF) and the four heat-shock proteins HSPA1B (heat shock 70kDa protein 1B), HSPA5 (heat shock

16

70kDa protein 5), HSP90B1 (heat shock protein 90kDa beta member 1), and HSPA9B (heat shock 70kDa protein 9). A similar trend was observed at 32 hours after treatment with 45% of upregulated genes being involved in anti-apoptotic processes and 18% showing pro-apoptotic potential. The proportion of upregulated pro- and anti-apoptotic genes at the two earlier time points after 4 h and 8 h of stimulation was more balanced and similar to the background distribution. The two anti-apoptotic genes HSPA1B and BAG3 were upregulated at all 4 time points (webtable 2). All of the anti-apoptotic genes listed above were also upregulated after 32 h of bortezomib treatment (webtable 2).

Strong Basal and Bortezomib-induced Hsp70 Protein Expression in PTC but not in GMC. Stress response or heat shock is a cellular adaptive response, which helps to maintain cellular homeostasis of living cells under stress. Among the many changes in cellular activity and physiology, the most remarkable event in stressed cells is the production of a highly conserved set of proteins, the Hsps or stress proteins (Arya et al., 2007). As we found several Hsp genes to be upregulated in bortezomib-stimulated PTC when compared with unstimulated controls, and as the heat shock 70 kDa protein 1B (HSPA1B) gene showed the highest upregulation in oligonucleotide microarray analysis (webtable 1; Fig. 7), we next investigated basal and bortezomib-induced protein expression of Hsp70 in PTC, LLC-PK$_1$ and GMC using Western blot analysis. Interestingly, in quiescent PTC and LLC-PK$_1$ a much higher basal Hsp70 protein expression was obtained when compared with GMC where very low basal Hsp70 protein expression was detected under identical conditions (Figs. 8 and 10). In addition, 50 nM bortezomib led to a strong and time-dependent additional induction of Hsp70 proteins in PTC, which started after 8 h and peaked after 36 h (Fig. 8). In contrast, bortezomib-induced Hsp70 protein expression was weaker in GMC (Figs. 8 and 10), and peaked after 24 h (Fig. 8).

Bortezomib Induces Upregulation of BAG3 mRNA and Downregulation of BAG5 mRNA in PTC. Proteins that share the BAG (Bcl-2-associated athanogene) domain were originally identified by their ability to associate with the anti-apoptotic protein Bcl-2 (Doong et al., 2002). BAG-family proteins were also found to interact with Hsp70 and are able to modulate, either positively or negatively, the functions of these chaperone proteins (Doong et al., 2002). BAG3, also known as CAIR-1 or Bis, has been reported to sustain cell survival and/or to downmodulate the apoptotic response in some cell types (Rosati et al., 2007). BAG5, on the other hand, represents the only BAG-family member with four BAG repeats and has been reported to enhance dopaminergic neuronal degeneration through inhibition of the E3 ligase activity of parkin and the chaperone activity of Hsp70 (Kalia et al., 2004). As we found evidence for upregulation of BAG3 and downregulation of BAG5 during microarray analysis of bortezomib-stimulated PTC when compared with untreated controls, we next studied mRNA expression of BAG3 and BAG5 in bortezomib-stimulated PTC using real-time PCR analysis. As depicted in Fig. 9A, 50 nM bortezomib led to a strong, 11.7-fold (n=6) and 10.6-fold (n=6) induction of BAG3 mRNA after 8 h and 16 h, respectively. The p-values of t-tests comparing the delta ct PCR values between treated and control samples were <0.001 at both time points. BAG5 mRNA expression, on the other hand, was significantly down-regulated after 8 h (0.61-fold; n=6) and 16 h (0.54-fold; n=6) of bortezomib treatment (p-values of 0.002 and <0.001 at the 8 h and 16 h time points, respectively) (Fig. 9B). The strong stimulatory effect of bortezomib on BAG3 expression was verified at the protein level in PTC and LLC-PK$_1$ when compared with a lower induction in GMC (Fig. 10). As these results corroborate the findings obtained in the oligonucleotide microarray assays it is tempting to speculate that bortezomib administration is not only able to induce genes which are able to sustain cell survival and/or to downmodulate apoptosis (e.g. BAG3 and Hsp70) but also to inhibit genes which might be involved in the induction of cell injury and/or cell death (e.g. BAG5).

Discussion

This study presents two major findings with relevance for both basic and applied clinical research of current applications of the proteasome inhibitor bortezomib in MM patients with renal impairment: 1. Bortezomib modulates renal cellular function in a cell type-specific manner. 2. In human proximal tubular cells (PTC), bortezomib affects a set of intracellular signaling mechanisms and genes which are likely to protect this renal epithelial cell type from apoptosis rather than inducing PTC apoptosis. Furthermore, our results are consistent with the idea that proteasome inhibitors in general, and specifically bortezomib, have the ability to act either as poisons, which induce apoptosis and cell death, or as remedies, which modulate cellular function (Wojcik, 1999; Meiners et al., 2008). Whereas rapidly proliferating cells with abnormal phenotypes are most sensitive to the proapoptotic action of proteasome inhibitors, differentiated cells are not or less sensitive, even when they form highly proliferating populations, such as bone marrow or epithelia. Different tumor cell lines also vary markedly in their sensitivity to proteasome inhibition, although the chymotrypsin-like activity of the 20S proteasome is inhibited to the same extent (Meiners et al., 2008). It is even possible to observe differential responsiveness to proteasome inhibition within the same cell type. A defined dose of proteasome inhibitors, for example, is capable of inducing apoptosis in proliferating but not in quiescent human leukemic HL60 cells (Drexler, 1997). Similar differential responsiveness to induction of apoptosis was observed in rat-1 fibroblasts, primary endothelial cells, and in tumor-derived lymphocytes and hepatocytes (in contrast to normal lymphocytes and hepatocytes) (Meiners et al., 2008). Whereas several mechanisms for proteasome inhibitor-mediated induction of apoptosis have been obtained and discussed, the molecular mechanisms of potential protective effects of proteasome inhibition in kidney cells are still largely unknown.

Bortezomib is currently used as chemotherapeutic drug because of its ability to block NF-κB, a transcription factor constitutively activated in many types of human cancer. Recent studies revealed reversibility of renal failure in newly diagnosed MM patients treated with high-dose dexamethasone containing regimens and a more rapid improvement of renal function in the presence of bortezomib (Nozza et al., 2006; Kastritis et al., 2007). We thus investigated direct cellular effects of bortezomib treatment and cell type-specific intracellular mechanisms induced by this proteasome inhibitor in PTC, LLC-PK$_1$ and GMC. We found evidence for distinct bortezomib-mediated protection pathways in PTC and LLC-PK$_1$ when compared with GMC. In the presence of bortezomib, PTC showed long-term activation of NF-κB signaling and long-term phosphorylation of Akt and ERK1/2 protein kinases, associated with lack of caspase-9, caspase-3 and apoptosis induction. In contrast, bortezomib led to a strong time-dependent activation of caspases-9 and -3 in GMC, which was followed by apoptosis induction after 24 h. Furthermore, GMC did not present long-term phosphorylation of NF-κB, Akt and ERK1/2 but showed reduced Akt protein expression at late time points after bortezomib administration suggesting that the activation of either one of these survival pathways in PTC could be involved in the resistance of these cells to bortezomib-induced apoptosis. The fact that almost identical results have been obtained in both PTC (HK-2 cells) and LLC-PK$_1$ cells strongly argues against a predominant involvement of E6 and E7 oncoproteins of HPV 16 in the observed processes in PTC (Figs. 4 and 10).

Our data are in line with a recent study showing that proteasome inhibitors induce cell death but activate NF-κB in endometrial carcinoma cells and primary explant culture of endometrial adenocarcinoma (Dolcet et al., 2006). In HepG2 cells, bortezomib also induced a decrease in IκB-α protein levels and concomitantly an increase in NF-κB DNA-binding activity (Calvaruso et al., 2006). In renal cell carcinoma (RCC), on the other hand, the maximum bortezomib-induced apoptosis depended on its NF-κB inhibitory effect and on NF-κB-independent mechanisms (An et al., 2004). Moreover, in several human gastric cancer cell

lines, bortezomib led to a significant growth inhibition, which was associated with a decrease in the activity of ERK1/2 and Akt signaling pathways and with increased p21 protein expression (Fujita et al., 2007). Interestingly, it has been reported recently that constitutive NF-κB activity in RCC cells is mediated, at least in part, through a signaling cascade consisting of epidermal growth factor (EGF) receptor, PI3K, and Akt (An and Rettig, 2007). Pretreatment with an EGF receptor tyrosine kinase inhibitor sensitized these cells to bortezomib-mediated cytotoxicity by inhibiting constitutive NF-κB activity (An and Rettig, 2007). In MM cells and in primary MM plasma cells, the combination of a Ras signaling pathway inhibitor with bortezomib induced a rapid, synergistic tumor cell death, which was associated with increased caspase-3, -8, and -9 cleavage and concomitant down-regulation of Akt phosphorylation (David et al., 2005). Interestingly, down-regulation of Akt phosphorylation was seen only in combination therapy and not observed with either single agent (David et al., 2005). In Jurkat lymphoblastic and U937 myelomonocytic leukemia cells, bortezomib resulted in the activation of c-Jun-N-terminal kinase (JNK) and p38 MAPK but in the inactivation of ERK1/2 associated with cytochrome c release, caspase-9, -8, and -3 activation, and apoptosis induction (Yu et al., 2004). Inducible expression of a constitutively active MEK1 construct blocked bortezomib-mediated ERK1/2 inactivation, significantly attenuated bortezomib-induced lethality and prevented JNK activation (Yu et al., 2004). These data are in line with our idea that bortezomib is able to induce long-term stimulation of NF-κB- and ERK1/2-driven protection pathways in PTC but not in GMC, and that this contributes to the decreased susceptibility of PTC to bortezomib-stimulated apoptosis.

In addition to the stimulation of survival signaling pathways, microarray experiments revealed evidence for a time-dependent shift of gene expression towards a predominance of anti-apoptotic genes in bortezomib-stimulated PTC. At the 16 h time point after bortezomib administration, ten upregulated genes were involved in anti-apoptotic processes whereas only three had pro-apoptotic activity. Although this result does not preclude that a single pro-

apoptotic gene could overcome the cumulative effect of a number of anti-apoptotic or pro-survival genes it is in line with the data derived from apoptosis assays. For Hsp70 and BAG3 the microarray results obtained in PTC were corroborated in two proximal tubular epithelial cell lines (PTC and LLC-PK$_1$) by Western blot (Figs. 8 and 10) and real-time PCR analysis (Fig. 9) and compared with GMC (Fig. 10). Furthermore, our results are supported by gene expression analysis of B-lymphoma cell lines with differential sensitivity to bortezomib. At concentrations that effectively inhibited proteasome activity, bortezomib-induced expression of Hsp27, Hsp70, Hsp90 and T-cell factor 4 was associated with bortezomib resistance, while overexpression of activating transcription factor 3 (ATF3), ATF4, ATF5, c-Jun, JunD and caspase-3 was associated with sensitivity to bortezomib-induced apoptosis (Shringarpure et al., 2006). In the hepatoma HepG2 cell line the expression of the survival factor Hsp72 also increased in 50 nM bortezomib-treated cells. After 24 h of stimulation with bortezomib, Hsp72 interacted with and sequestered the pro-apoptotic factors p53, AIF, Bax and Apaf-1 in HepG2 cells (Calvaruso et al., 2007). Although the nuclear levels of Hsp72, p53 and AIF steadily increased, the interaction of Hsp72 with these factors diminished during the second day of treatment, which was associated with the activation of caspases (Calvaruso et al., 2007). All together our data obtained in PTC when compared with GMC suggest that induction of Hsp70 mRNA and protein expression could be involved in the relative resistance of these human proximal tubular cells against bortezomib-induced apoptosis. This idea is further supported by the finding of a strong bortezomib-induced stimulation of BAG3 mRNA and protein expression in PTC and LLC-PK$_1$ (Figs. 9 and 10). Expression of BAG3 is elevated in some leukemia and solid tumors and antisense-mediated reductions in BAG3 expression enhances the apoptotic response to chemotherapeutic drugs in some malignant cells (Rosati et al., 2007). Most recently it has been reported that BAG3 was induced at the transcriptional level by proteasome inhibitors such as MG132 and lactacystin in cancer cell lines derived from different histology (Wang et al., 2008). Prohibition of BAG3 upregulation

using small interfering RNAs enhanced cytotoxicity induced by MG132, suggesting that induction of BAG3 might be an adaptive response to proteasome inhibition (Wang et al., 2008). The time-dependent massive bortezomib-stimulated expression of BAG3 mRNA levels in PTC supports these results. BAG5 mRNA expression, on the other hand, is inhibited by bortezomib treatment in PTC. This BAG family member has been reported to enhance dopaminergic neuronal degeneration through inhibition of the E3 ligase activity of parkin and the chaperone activity of Hsp70 (Kalia et al., 2004).

In summary, it is tempting to speculate that both bortezomib-stimulated transcription of cell protection genes and bortezomib-inhibited transcription of pro-apoptotic genes might support NF-κB, Akt/PKB and/or ERK1/2 pro-survival signaling pathways in order to reduce or delay apoptotic cell death in PTC. Identification of bortezomib-induced survival genes might yield novel therapeutic approaches for the stimulation of early proximal tubulointerstitial protection to avoid renal disease progression. Finally the concept of bortezomib representing a blocker of both NF-κB activation and cell survival should be carefully examined in particular renal cell types.

Acknowledgements

JPET #142604

References

Adams J (2002) Proteasome inhibitors as new anticancer drugs. *Curr Opin Oncol* 14: 628-634.

An J, Rettig MB (2007) Epidermal growth factor receptor inhibition sensitizes renal cell carcinoma cells to the cytotoxic effects of bortezomib. *Mol Cancer Ther* **6:** 61-69.

An J, Sun Y, Fisher M, Rettig MB (2004) Maximal apoptosis of renal cell carcinoma by the proteasome inhibitor bortezomib is nuclear factor-κB dependent. *Mol Cancer Ther* **3:** 727-736.

Arya R, Mallik M, Lakhotia S (2007) Heatshock genes – integrating cell survival and death. *J Biosci* **32:** 595-610.

Batuman V (2007) Proximal tubular injury in myeloma. *Contrib Nephrol* **153:** 87-104.

Brazma A, Hingamp P, Quackenbush J, Sherlock G, Spellman P, Stoeckert C, Aach J, Ansorge W, Ball CA, Causton HC, Gaasterland T, Glenisson P, Holstege FC, Kim IF, Markowitz V, Matese JC, Parkinson H, Robinson A, Sarkans U, Schulze-Kremer S, Stewart J, Taylor R, Vilo J, Vingron M (2001) Minimum information about a microarray experiment (MIAME)-toward standards for microarray data. *Nat Genet* **29:** 365-371.

Calvaruso G, Giuliano M, Portanova P, De Blasio A, Vento R, Tesoriere G (2006) Bortezomib induces in HepG2 cells IκBα degradation mediated by caspase-8. *Mol Cell Biochem* **287:** 13-19.

Calvaruso G, Giuliano M, Portanova P, Pellerito O, Vento R, Tesoriere G (2007) Hsp72 controls bortezomib-induced HepG2 cell death via interaction with pro-apoptotic factors. *Oncol Rep* **18:** 447-450.

Chanan-Khan AA, Kaufman JL, Mehta J, Richardson PG, Miller KC, Lonial S, Munshi NC, Schlossman R, Tariman J, Singhal S (2007) Activity and safety of bortezomib in multiple myeloma patients with advanced renal failure: A multicenter retrospective study. *Blood* **109:** 2604-2606.

Ciechanover A, Schwartz AL (1998) The ubiquitin-proteasome pathway: The complexity and myriad functions of proteins death. *Proc Natl Acad Sci USA* **95:** 2727-2730.

Cusack JC Jr, Liu R, Houston M, Abendroth K, Elliott PJ, Adams J, Baldwin AS Jr (2001) Enhanced chemosensitivity to CPT-11 with proteasome inhibitor PS-341: Implications for systemic nuclear factor-κB inhibition. *Cancer Res* **61:** 3535-3540.

Dai Y, Rahmani M, Grant S (2003) Proteasome inhibitors potentiate leukemic cell apoptosis induced by the cyclin-dependent kinase inhibitor flavopiridol through a SAPK/JNK- and NF-kappaB-dependent process. *Oncogene* **22:** 7108-7122.

David E, Sun S-Y, Waller EK, Chen J, Khuri FR, Lonial S (2005) The combination of the farnesyl transferase inhibitor lonafarnib and the proteasome inhibitor bortezomib induces synergistic apoptosis in human myeloma cells that is associated with down-regulation of p-Akt. *Neoplasia* **106:** 4322-4329.

DeMartino GN, Gillette TG (2005) Proteasomes: Machines for all reasons. *Cell* **129:** 659-662.

Dolcet X, Llobet D, Encinas M, Pallares J, Cabero A, Schoenenberger JA, Comella JX, Matias-Guiu X (2006) Proteasome inhibitors induce death but activate NF-κB on endometrial carcinoma cell lines and primary culture explants. *J Biol Chem* **281:** 22118-22130.

Doong H, Vrailas A, Kohn EC (2002) What's in the "BAG"? – a functional domain analysis of the BAG-family of proteins. *Cancer Lett* **188:** 25-32.

Drexler HC (1997) Activation of the cell death program by inhibition of proteasome function. *Proc Natl Acad Sci USA* **94:** 855-860.

Frankel A, Man S, Elliott P, Adams J, Kerbel KS (2000) Lack of multicellular drug resistance observed in human ovarian and prostate carcinoma treated with the proteasome inhibitor PS-341. *Clin Cancer Res* **6:** 3719-3728.

Fujita T, Doihara H, Washio K, Ino H, Murakami M, Naito M, Shimizu N (2007) Antitumor effects and drug interactions of the proteasome inhibitor bortezomib (PS341) in gastric cancer cells. *Anticancer Drugs* **18:** 677-686.

Hideshima T, Richardson P, Chauhan D, Palombella VJ, Elliott PJ, Adams J, Anderson KC (2001) The proteasome inhibitor PS-341 inhibits growth, induces apoptosis, and overcomes drug resistance in human multiple myeloma cells. *Cancer Res* **61:** 3071-3076.

Jagannath S, Durie BG, Wolf J, Camacho E, Irwin D, Lutzky J, McKinley M, Gabayan E, Mazumder A, Schenkein D, Crowley J (2005) Bortezomib therapy alone and in combination with dexamethasone for previously untreated symptomatic multiple myeloma. *Br J Haematol* **129:** 776-783.

Kalia SK, Lee S, Smith PD, Liu L, Crocker SJ, Thorarinsdottir TE, Glover JR, Fon EA, Park DS, Lozano AM (2004) BAG5 inhibits parkin and enhances dopaminergic neuron degeneration. *Neuron* **44:** 931-945.

Kastritis E, Anagnostopoulos A, Roussou M, Gika D, Matsouka C, Barmparousi D, Grapsa I, Psimenou E, bamias A, Dimopoulos MA (2007) Reversibility of renal failure in newly diagnosed multiple myeloma patients treated with high dose dexamethasone-containing regimes and the impact of novel agents. *Haemtologica* **92:** 546-549.

Livak KJ, Schmittgen TD (2001) Analysis of relative gene expression data using real-time quantitative PCR and the 2(-Delta Delta C(T)) *Method Methods* **25:** 402-408.

Manning BD, Cantley LC (2007) AKT/PKB signaling: navigating downstream. *Cell* **129:** 1261-1274.

Meiners S, Ludwig A, Stangl V, Stangl K (2008) Proteasome inhibitors: Poisons and remedies. *Med Res Rev* **28:** 309-327.

Mohrbacher A, Levine AM (2005) Reversal of advanced renal dysfunction on bortezomib treatment in multiple myeloma patients. *Am Soc Clin Oncol Meeting Proc* **24:** 6714. (Abstract)

Nozza A, Siracisano L, Armando S (2006) Bortezomib-dexamethasone combination in a patient with refractory multiple myeloma and impaired renal function. *Clin Ther* **28:** 953-959.

Ostermann E, Schrattbauer K, Ludwig H, Graf H (2006) Rapid recovery of kidney function in patients with multiple myeloma under bortezomib-combination therapy. *J Am Soc Nephrol* **17:** 808A. (Abstract)

Perkins ND (2007) Integrating cell-signalling pathways with NF-κB and IKK function. *Nature Rev* **8:** 49-62.

Rosati A, Ammirante M, Gentilella A, Basile A, Festa M, Pascale M, Marzullo L, Belisario MA, Tosco A, Franceschelli S, Moltedo O, Pagliuca G, Lerose R, Turco MC (2007) Apoptosis inhibition in cancer cells: a novel molecular pathway that involves BAG3 protein. *Int J Biochem Cell Biol* **39:** 1337-1342.

Sarközi R, Miller B, Pollack V, Feifel E, Mayer G, Sorokin A, Schramek H (2007) ERK1/2-driven and MKP-mediated inhibition of EGF-induced ERK5 signaling in human proximal tubular cells. *J Cell Physiol* **211:** 88-100.

Schramek H, Gstraunthaler G, Willinger CC, Pfaller W (1993) Hyperosmolality regulates endothelin release by Madin-Darby Canine Kidney cells. *J Am Soc Nephrol* **4:** 206-213.

Schramek H, Schuhmacher M, Pfaller W (2006) Sustained ERK-2 activation in rat glomerular mesangial cells: differential regulation by protein phosphatases. *Am J Physiol Renal Physiol* **271:** F423-F432.

Shringarpure R, Catley L, Bhole D, Burger R, Podar K, Tai Y-T, Kessler B, Galardy P, Ploegh H, Tassone P, Hideshima T, Mitsiades C, Munshi NC, Chauhan D, Anderson KC (2006) Gene expression analysis of B-lymphoma cells resistant and sensitive to bortezomib. *Br J Haematol* **134:** 145-156.

Tori S, Yamamoto Y, Tsuchiya Y, Nishida E (2006) ERK MAP kinase in G1 cell cycle progression and cancer. *Cancer Sci* **97:** 697-702.

Traenckner EB, Wilk S, Baeuerle PA (1994) A proteasome inhibitor prevents activation of NF-kappa B and stabilizes a newly phosphorylated form of I kappa B-alpha that is still bound to NF-kappa B. *EMBO J* **13:** 5433-5441.

Wang H-Q, Liu H-M, Zhang H-Y, Guan Y, Du Z-X (2008) Transcriptional upregulation of BAG3 upon proteasome inhibition. *Biochem Biophy Res Commun* **365:** 381-385.

Wojcik C (1999) Proteasomes in apoptosis: Villains or guardians? *Cell Mol Life Sci* **56:** 908-917.

Yu C, Rahmani M, Dent P, Grant S (2004) The hierarchical relationship between MAPK signaling and ROS generation in human leukemia cells undergoing apoptosis in response to the proteasome inhibitor bortezomib. *Exp Cell Res* **295:** 555-566.

JPET #142604

Footnotes

Reprint requests to: Dr. Herbert Schramek, Division of Nephrology and Hypertension, Department of Internal Medicine IV, Innsbruck Medical University, Anichstrasse 35, A-6020 Innsbruck, Austria. E-mail: herbert.schramek@i-med.ac.at

JPET #142604

Legends for Figures

Figure 1. Bortezomib-induced effects on apoptosis and necrosis in PTC when compared with GMC. (A) Effect of 50 nM bortezomib on apoptosis in PTC and in GMC after 24 h of stimulation when compared with untreated controls. (B) Effect of 50 nM bortezomib on necrosis in PTC and in GMC after 24 h of stimulation when compared with untreated controls. PTC and GMC were stained with a FITC-conjugated Annexin-V and propidium iodide for 10 minutes and were then subjected to flow cytometric analysis as outlined in the "Materials and Methods" section. Representative dotblots of Annexin-V/propidium iodide staining of PTC and GMC are depicted in (C) and (D), respectively.

Figure 2. Bortezomib-induced time-dependent activation of caspase-9 and caspase-3 in GMC when compared with PTC. PTC and GMC were serum- and supplement-starved for 48 h and were then exposed to 50 nM bortezomib for 8, 12, 16, 24, 36 h when compared with untreated controls (8 and 36 h). Protein matched samples of stimulated cells and unstimulated controls were separated on SDS 10% PAGE and analyzed by Western immunoblot for cleaved-caspase-9, cleaved-caspase-3 and ß-actin protein expression. The results from one representative Western blot of n=5 separate experiments are depicted.

Figure 3. Bortezomib-induced time-dependent degradation of IκB-α and phosphorylation of NF-κBp65 in PTC when compared with GMC. PTC and GMC were serum- and supplement-starved for 48 h and were then exposed to 50 nM bortezomib for 8, 12, 16, 24, 36 h when compared with untreated controls (8 and 36 h). Protein matched samples of stimulated cells and unstimulated controls were separated on SDS 10% PAGE and analyzed by Western immunoblot for IκB-α protein expression, NF-κBp65 serine 536 phosphorylation, and NF-κBp65 protein expression. The results from one representative Western blot of n=5 separate experiments are depicted.

Figure 4. Effects of bortezomib on caspase-3 activation, IκB-α degradation and NF-κBp65 phosphorylation in the proximal tubular cell line LLC-PK$_1$. PTC, LLC-PK$_1$ cells, and GMC were serum- and supplement-starved for 48 h and were then exposed to 50 nM bortezomib for 24 h when compared with untreated controls. Protein matched samples of stimulated cells and unstimulated controls were separated on SDS 10% PAGE and analyzed by Western immunoblot for cleaved-caspase-3 expression, ß-actin protein expression, IκB-α protein expression, NF-κBp65 serine 536 phosphorylation, and NF-κBp65 protein expression. The results from one representative Western blot of n=4 separate experiments are depicted. C, unstimulated control; B, bortezomib-stimulated.

Figure 5. Time-dependent effects of bortezomib on Akt1/2/3 phosphorylation and Akt1/2/3 protein expression in PTC when compared with GMC. PTC and GMC were serum- and supplement-starved for 48 h and were then exposed to 50 nM bortezomib for 8, 12, 16, 24, 36 h when compared with untreated controls (8 and 36 h). Protein matched samples of stimulated cells and unstimulated controls were separated on SDS 10% PAGE and analyzed by Western immunoblot for Akt1/2/3 phosphorylation, Akt1/2/3 protein expression, and ß-actin protein expression. The results from one representative Western blot of n=3 separate experiments are depicted.

Figure 6. Time-dependent effects of bortezomib on ERK1/2 phosphorylation and ERK1/2 protein expression in PTC when compared with GMC. PTC and GMC were serum- and supplement-starved for 48 h and were then exposed to 50 nM bortezomib for 8, 12, 16, 24, 36 h when compared with untreated controls (8 and 36 h). Protein matched samples of stimulated cells and unstimulated controls were separated on SDS 10% PAGE and analyzed by Western immunoblot for ERK1/2 phosphorylation, and ERK1/2 protein expression. The results from one representative Western blot of n=3 separate experiments are depicted.

Figure 7. Distribution of differentially expressed pro-apoptotic (black), anti-apoptotic (grey), and apoptosis-related (white) genes 16 hours after bortezomib treatment when compared with the reference set. Gene expression log2 R/G values are depicted in detail for up- and down-regulated anti- and pro-apoptotic genes. HGNC Gene Symbols are used for gene annotation.

Figure 8. Time-dependent effects of bortezomib on Hsp70 protein expression in PTC when compared with GMC. PTC and GMC were serum- and supplement-starved for 48 h and were then exposed to 50 nM bortezomib for 8, 12, 16, 24, 36 h when compared with untreated controls (8 and 36 h). Protein matched samples of stimulated cells and unstimulated controls were separated on SDS 10% PAGE and analyzed by Western immunoblot for Hsp70 and ß-actin protein expression. The results from one representative Western blot of n=3 separate experiments are depicted.

Figure 9. Bortezomib-induced effects on BAG3 mRNA expression and on BAG5 mRNA expression in PTC. PTC were serum- and supplement-starved for 48 h and were then exposed to 50 nM bortezomib for 8 and 16 h when compared with untreated controls (8 and 16 h). Thereafter, total RNA was isolated and used for real-time PCR analysis. (A) cDNAs from six independent RNA isolations were applied for real-time PCR analysis of the BAG3 gene. Data are presented as fold change above BAG3 mRNA control levels after normalizing to GAPDH expression. Each data point indicates the average of n=6 independent experiments with error bars corresponding to SEM. (B) cDNAs from six independent RNA isolations were applied for real-time PCR analysis of the BAG5 gene. Data are presented as fold change when compared with BAG5 mRNA control levels after normalizing to GAPDH expression. Each data point indicates the average of n=6 independent experiments with error bars corresponding to SEM.

Figure 10. Bortezomib-induced effects on Hsp70 and BAG3 protein expression in PTC, LLC-PK$_1$, and GMC. Cells were serum- and supplement-starved for 48 h and were then

exposed to 50 nM bortezomib for 24 h when compared with untreated controls. Protein

matched samples of stimulated cells and unstimulated controls were separated on SDS 10%

PAGE and analyzed by Western immunoblot for Hsp70, BAG3, and ß-actin protein

expression. The results from one representative Western blot of n=2 separate experiments are

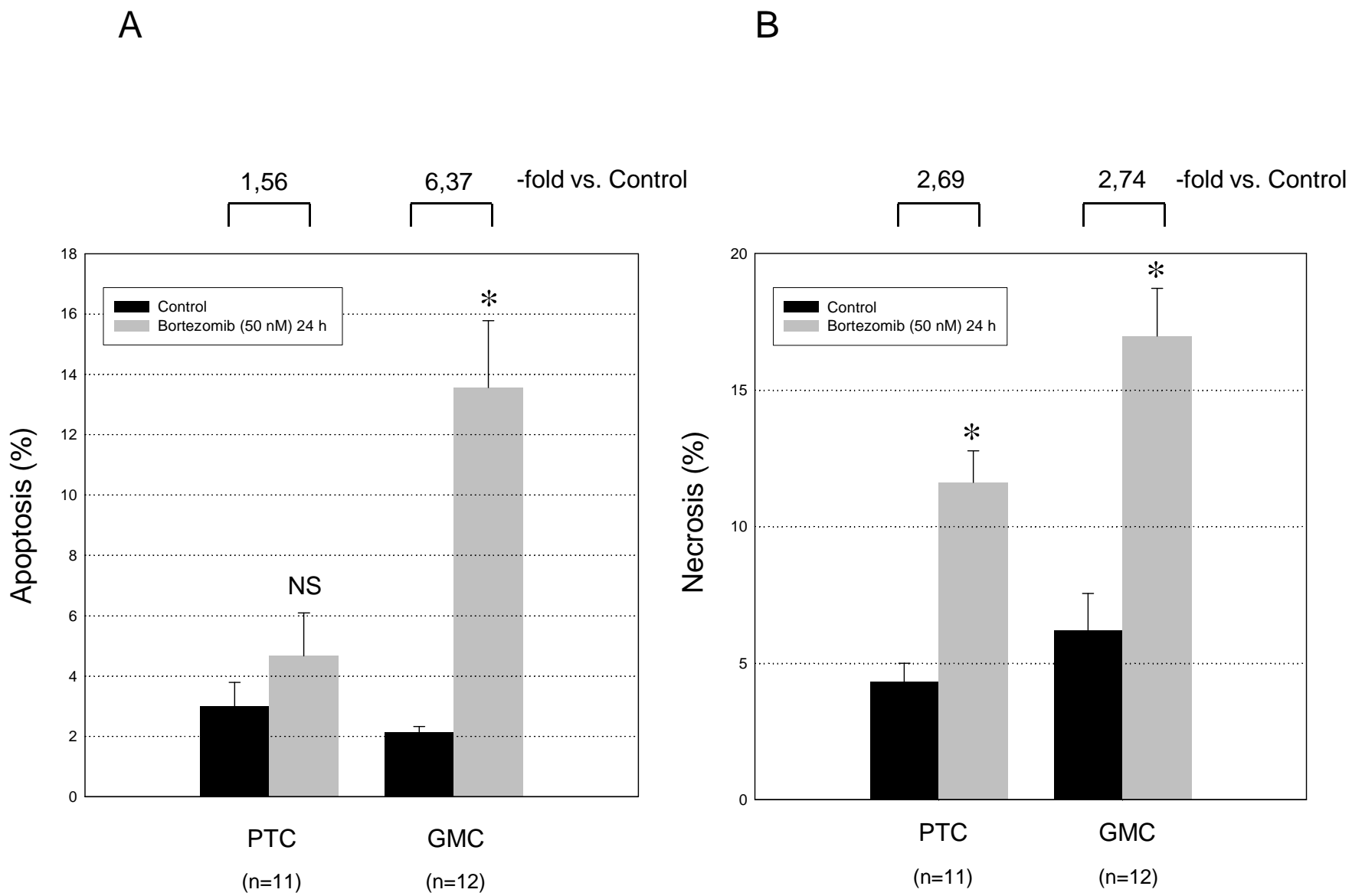depicted. C, unstimulated control; B, bortezomib-stimulated.
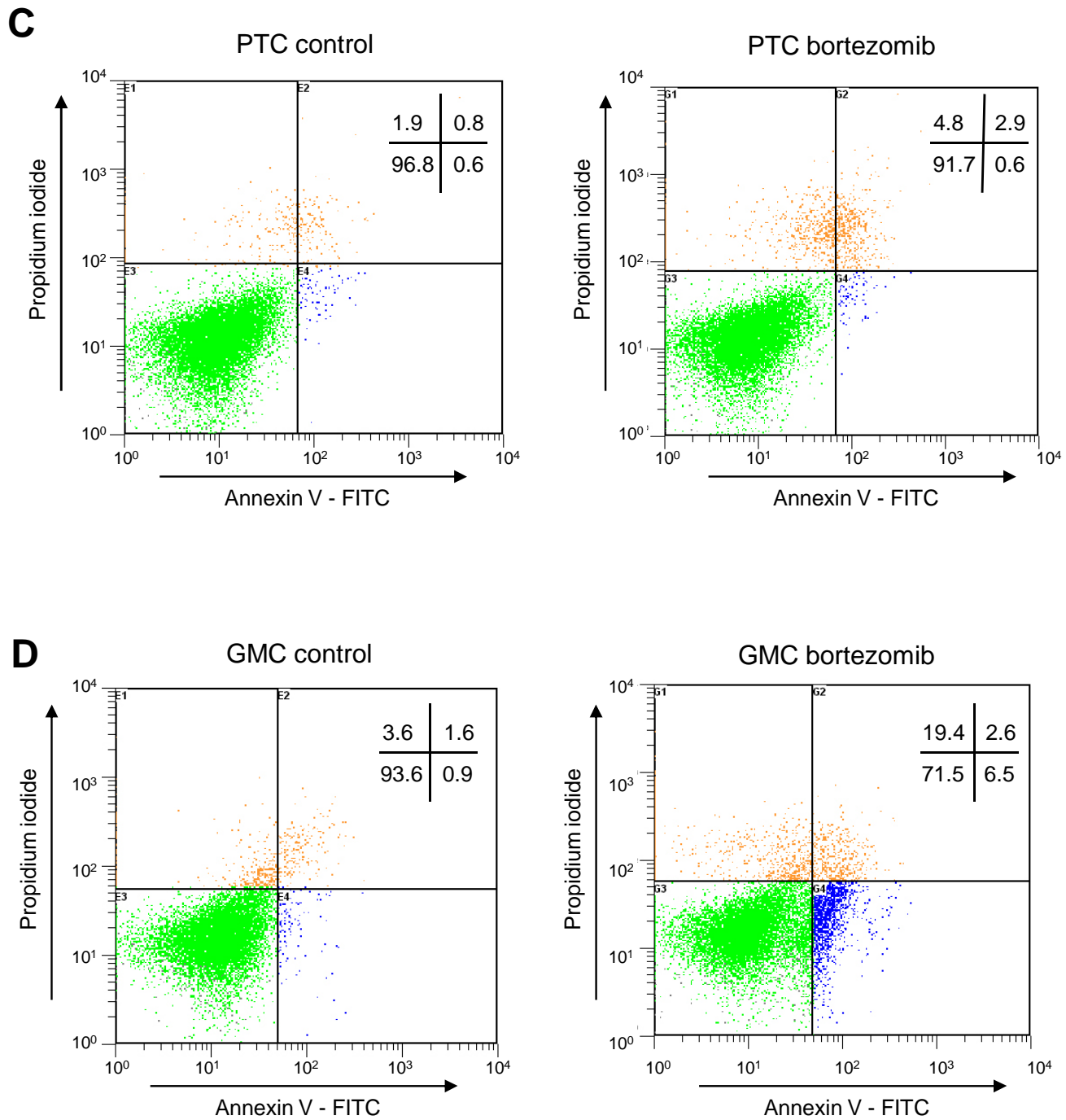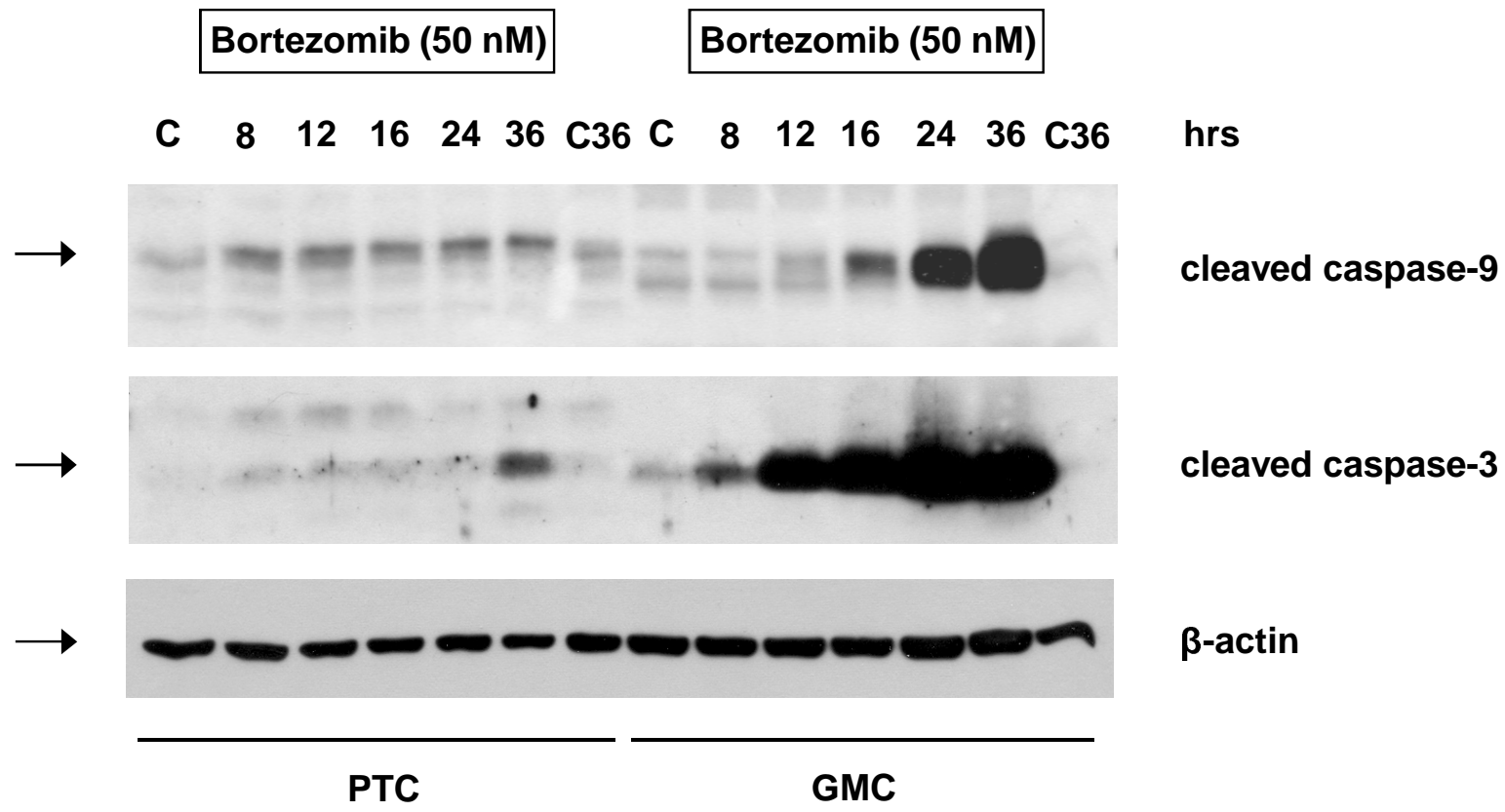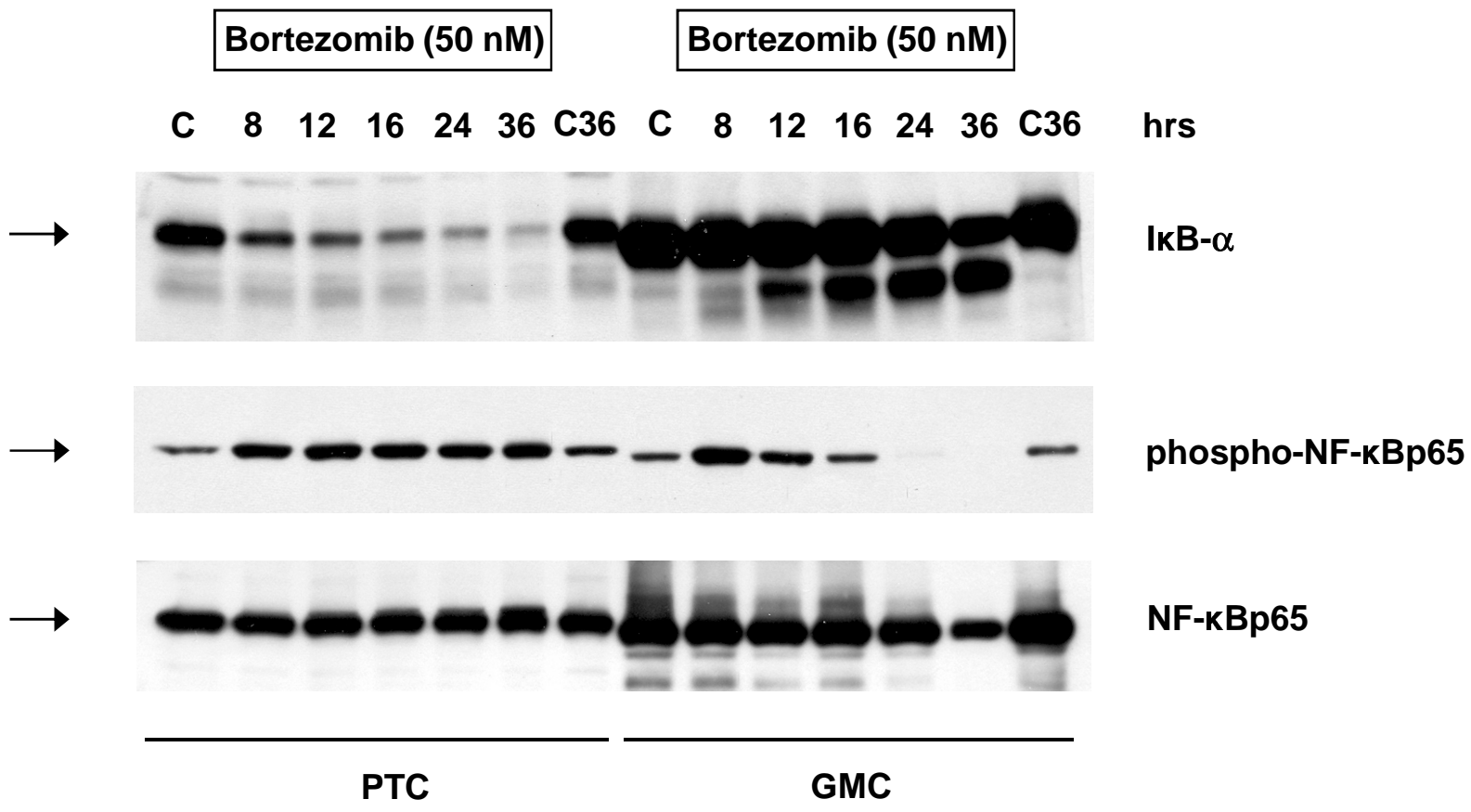
Fig. 1

C

PTC control

1.9	0.8
96.8	0.6

PTC bortezomib

4.8	2.9
91.7	0.6

D

GMC control

3.6	1.6
93.6	0.9

GMC bortezomib

19.4	2.6
71.5	6.5

Fig. 1

Bortezomib (50 nM)　　　**Bortezomib (50 nM)**

C　8　12　16　24　36　C36　C　8　12　16　24　36　C36　**hrs**

→　**cleaved caspase-9**

→　**cleaved caspase-3**

→　**β-actin**

PTC　　　　　　　　　　GMC

Fig. 2

	Bortezomib (50 nM)						Bortezomib (50 nM)							
C	8	12	16	24	36	C36	C	8	12	16	24	36	C36	hrs

IκB-α

phospho-NF-κBp65

NF-κBp65

PTC   GMC

Fig. 3

Fig. 4

	Bortezomib (50 nM)							Bortezomib (50 nM)						

| C | 8 | 12 | 16 | 24 | 36 | C36 | C | 8 | 12 | 16 | 24 | 36 | C36 | hrs |

→ phospho-Akt

→ Akt 1/2/3

→ ß-actin

PTC   **GMC**

Fig. 5

Bortezomib (50 nM)   **Bortezomib (50 nM)**

C   8   12   16   24   36   C36   C   8   12   16   24   36   C36   hrs

phospho-ERK1/2

ERK 1
ERK 2

PTC   GMC

Fig. 6

Fig. 7

Bortezomib (50 nM) **Bortezomib (50 nM)**

| C | 8 | 12 | 16 | 24 | 36 | C36 | C | 8 | 12 | 16 | 24 | 36 | C36 | hrs |

→ **Hsp 70**

→ **ß-actin**

PTC   GMC

Fig. 8

A

BAG3 mRNA (n=6)

B

BAG5 mRNA (n=6)

Fig. 9

Fig. 10